Multiscale Discontinuous Galerkin Methods for Elliptic Problems with Multiple Scales

Jørg Aarnes[1] and Bjørn–Ove Heimsund[2]

[1] SINTEF Applied Mathematics, PB. 124, 0314 Oslo, Norway.
Jorg.Aarnes@sintef.no
[2] University of Bergen, Allégaten 41, 5007 Bergen, Norway.
Bjorn-Ove.Heimsund@cipr.uib.no

Summary. We introduce a new class of discontinuous Galerkin (DG) methods for solving elliptic problems with multiple scales arising from e.g., composite materials and flows in porous media. The proposed methods may be seen as a generalization of the multiscale finite element (FE) methods. In fact, the proposed DG methods are derived by combining the approximation spaces for the multiscale FE methods and relaxing the continuity constraints at the inter-element interfaces. We demonstrate the performance of the proposed DG methods through numerical comparisons with the multiscale FE methods for elliptic problems in two dimensions.

Key words: multiscale methods, discontinuous Galerkin methods, elliptic partial differential equations

1 Introduction

We consider solving the second-order elliptic equation

$$\begin{cases} -\nabla \cdot (a(x)\nabla u) = f, & \text{in } \Omega \subset \mathcal{R}^{\mathrm{d}}, \\ u = 0, & \text{on } \Gamma_{\mathrm{D}} \subset \partial\Omega, \\ -a(x)\nabla u \cdot n = 0, & \text{on } \Gamma_{\mathrm{N}} = \partial\Omega \backslash \Gamma_{\mathrm{D}}, \end{cases} \tag{1}$$

where Ω is bounded, $\partial\Omega$ is Lipschitz, n is the outward unit normal on $\partial\Omega$ and $a(x) = (a_{ij}(x))$ is a symmetric positive definite tensor with uniform upper and lower bounds:

$$0 < \alpha|y|^2 \leq y^T a(x) y \leq \beta|y|^2 < \infty, \quad \forall x \in \Omega,\ \forall y \in \mathcal{R}^d,\ y \neq 0.$$

We will interpret the variable u as the (flow) potential and q as the (flow) velocity. The homogeneous boundary conditions are chosen for presentational brevity. General boundary conditions can be handled without difficulty.

Equation (1) may represent incompressible single-phase porous media flow or steady state heat conduction through a composite material. In single-phase flow, u

is the flow potential, $q = -a(x)\nabla u$ is the Darcy filtration velocity and $a(x)$ is the (rock) permeability of the porous medium. For heat conduction in composite materials, u, q and $a(x)$ represents temperature, heat flow density, and thermal conductivity respectively. These are typical examples of problems where $a(x)$ can be highly oscillatory and the solution of (1) displays a multiscale structure. This leads to some fundamental difficulties in the development of robust and reliable numerical models.

In this paper we introduce a new class of DG methods for solving this particular type of multiscale elliptic problems. Until recently, DG methods have been used mainly for solving partial differential equations of hyperbolic type, see e.g. [10] for a comprehensive survey of DG methods for convection dominated problems. Indeed, whereas DG methods for hyperbolic problems have been subject to active research since the early seventies, it is only during the last decade or so that DG methods have been applied to purely elliptic problems, cf. [5] and the references therein. The primary motivation for applying DG methods to elliptic problems is perhaps their flexibility in approximating rough solutions that may occur in elliptic problems arising from heterogeneous and anisotropic materials. However, to our knowledge, previous research on DG methods for elliptic problems has been confined to solving elliptic partial differential equations with smooth coefficients.

DG methods approximate the solution to partial differential equations in finite dimensional spaces spanned by piecewise polynomial base functions. As such, they resemble the FE methods, but, unlike the FE methods, no continuity constraints are explicitly imposed at the inter-element interfaces. This implies that the weak formulation subject to discretization must include jump terms across interfaces and that some artificial penalty terms must be added to control the jump terms. On the other hand, the weak continuity constraints give DG methods a flexibility which allows a simple treatment of, e.g., unstructured meshes, curved boundaries and h- and p-adaptivity. Another key feature with DG methods is their natural ability to impose mass conservation locally. Moreover, the "local" formulation of the discrete equations allows us us to use grid cells of arbitrary shapes without difficulty. We may therefore choose the gridlines to be aligned with sharp contrasts in, for instance, underlying heterogeneous materials.

The multiscale FE methods (MsFEMs) introduced in [9, 12] have been successfully applied to multiscale elliptic problems, but their accuracy is to some degree sensitive to the selection of the boundary conditions that determine the FE base functions. If, for instance, strong heterogeneous features penetrate the inter-cell interfaces, then simple, e.g. linear, boundary conditions may be inadequate. In such situations, oversampling strategies or other techniques for the generation of adaptive boundary conditions must be used to recover the desired order of accuracy. This sensitivity to the selection of boundary conditions is partly due to the strong continuity requirements at the inter-element interfaces implicit in the FE methods.

Here we propose a class of multiscale DG methods (MsDGMs) for solving elliptic problems with multiple scales. One of the primary motives for developing MsDGMs is to generate multiscale methods that are less sensitive to the selection of boundary conditions for the base functions than is the case for the MsFEMs. Another nice feature with MsDGMs is that they produce solutions for both the potential

variable (e.g. pressure or temperature) and the velocity variable (e.g. phase velocity or thermal flux density) that reflect important subgrid variations in the elliptic coefficients. We will demonstrate the benefit of using multiscale methods in comparison with ordinary monoscale numerical methods and perform numerical experiments to display the performance of the MsDGMs relative to the original and mixed MsFEMs. We therefore attempt to reveal that there is a need for multiscale methods, and to demonstrate under what circumstances it may be advantageous to relax the inter-element continuity assumptions implicit in the MsFEMs.

The paper is organized as follows. We give the general mathematical setting for the DG methods in Sect. 2 and show how they are related to the more familiar FE methods. In particular we show that both standard and mixed FE methods may be viewed as special DG methods. This observation allows us to extend this type of FE methods to corresponding DG methods. In Sect. 3 we outline the MsFEMs introduced in [12] and [9] and exploit the relationship between FE methods and DG methods to derive a corresponding class of MsDGMs. Finally, Sect. 4 contains the numerical experiments and we conclude with a discussion of the results in Sect. 5.

2 Mathematical Formulations

In Sect. 2.1 we give the mathematical formulation of the DG methods for (1) and discuss the selection of the so-called numerical fluxes that are used to force weak continuity of the solution across inter-element interfaces. In Sect. 2.2 we show how the conforming and mixed FE methods may be viewed as special DG methods, and describe how such FE methods can be extended to corresponding DG methods.

2.1 Discontinuous Galerkin Methods

To define the DG methods we split (1) into the first order system,

$$\begin{aligned} q &= -a(x)\nabla u, && \text{in } \Omega, \\ \nabla \cdot q &= f, && \text{in } \Omega, \\ u &= 0, && \text{on } \Gamma_{\mathrm{D}}, \\ q \cdot n &= 0, && \text{on } \Gamma_{\mathrm{N}}. \end{aligned}$$

Furthermore, define the following approximation spaces:

$$\begin{aligned} Q_N &= \{p \in (H^1(\Omega))^d : p \cdot n = 0 \text{ on } \Gamma_N\}, \\ U_D &= \{v \in H^1(\Omega) : v = 0 \text{ on } \Gamma_D\}. \end{aligned}$$

Upon integration by parts, we now deduce the weak formulation: Find $q \in Q_N$ and $u \in U_D$ such that

$$\int_\Omega a^{-1} q \cdot p \,\mathrm{d}x = \int_\Omega u \nabla \cdot p \,\mathrm{d}x \qquad \forall p \in Q_N,$$

$$\int_\Omega q \cdot \nabla v \,\mathrm{d}x = -\int_\Omega f v \,\mathrm{d}x \qquad \forall v \in U_D.$$

In the DG methods, a similar set of equations is derived for each grid cell. However, for the grid cell equations it is not natural to impose homogeneous boundary conditions. The boundary conditions are therefore approximated from neighboring values of the unknown solution. Essentially we want to ensure that the potential u and the velocity q are "almost" continuous at the interfaces. Since we do not want to enforce continuity by imposing constraints on the approximation spaces as the FE methods do, we have to penalize the deviation from continuity by introducing an artificial penalty term. To understand the mechanism behind the penalty term, we digress for a moment in order to consider an example that illustrates the basic principle.

Example: Consider the Poisson equation with Dirichlet data,

$$\begin{cases} -\Delta u = f, \text{ in } \Omega, \\ \quad u = g, \text{ on } \partial\Omega, \end{cases}$$

and for each $\epsilon > 0$, let $u_\epsilon \in H^1(\Omega)$ be the solution to the regularized problem

$$\int_\Omega \nabla u_\epsilon \cdot \nabla v \,\mathrm{d}x + \int_{\partial\Omega} \frac{1}{\epsilon}(u_\epsilon - g)v \,\mathrm{d}s = \int_\Omega f v \,\mathrm{d}x \quad \forall v \in H^1(\Omega). \tag{2}$$

Here ds denotes the surface area measure. This problem corresponds to perturbing the boundary data so that instead of $u = g$ we have $u + \epsilon\nabla u \cdot n = g$ on $\partial\Omega$. One can show that (2) is well posed and that $u_\epsilon \to u \in H_0^1(\Omega)$ as $\epsilon \to 0$ [14]. Hence, we see that the extra penalty term is added in order to force, in the limit $\epsilon \to 0$, the satisfaction of the boundary conditions.

Just as the satisfaction of the Dirichlet boundary data was imposed weakly in (2), so can inter-element continuity be attained in a similar fashion. It was this observation that originally led to the development of the interior penalty (IP) methods [4, 11, 16]. Arnold et al. [5] recently recognized that the IP methods, along with several other methods with discontinuous approximation spaces, can be classified as DG methods. These methods differ in the flux approximating schemes used to force continuity at the inter element interfaces. We now describe the general framework for the DG methods with respect to the elliptic problem (1).

Let $\mathcal{T}(\Omega) = \{T \in \mathcal{T}\}$ be a family of elements in a partitioning of Ω and define $\partial\mathcal{T} = \cup\{\partial T : T \in \mathcal{T}\}$, $\Gamma = \partial\mathcal{T}\backslash\partial\Omega$ and $\Gamma_{ij} = \partial T_i \cap \partial T_j$, $T_i, T_j \in \mathcal{T}$. Next, introduce an approximation space $Q^h \times U^h \subset (H^1(\mathcal{T}))^d \times H^1(\mathcal{T})$ where

$$H^k(\mathcal{T}) = \{w \in L^2(\Omega) : w \in H^k(T), \forall T \in \mathcal{T}\}.$$

The DG method then seeks $q^h \in Q_N^h = Q^h \cap Q_N$ and $u^h \in U_D^h = U^h \cap U_D$ such that

$$\int_T a^{-1} q^h \cdot p \,\mathrm{d}x = \int_T u^h \nabla \cdot p \,\mathrm{d}x - \int_{\partial T} \bar{u}\, p \cdot n_T \,\mathrm{d}s \qquad \forall p \in Q_N^h, \tag{3}$$

$$\int_T q^h \cdot \nabla v \,\mathrm{d}x = -\int_T f v \,\mathrm{d}x + \int_{\partial T} v\, \bar{q} \cdot n_T \,\mathrm{d}s \qquad \forall v \in U_D^h, \tag{4}$$

for all $T \in \mathcal{T}$. Here n_T is the outward unit normal on ∂T and $(\bar{q}, \bar{u})$ are the so called numerical fluxes which represent an approximation to (q, u) on ∂T.

The Numerical Fluxes

The perhaps simplest and most natural choice of numerical fluxes is to set

$$(\bar{q}, \bar{u}) = \frac{1}{2}\left[(q^h, u^h)|_{T_i} + (q^h, u^h)|_{T_j}\right] \quad \text{on } \Gamma_{\text{ij}}.$$

We see that this option, which was considered by Bassi and Rebay in [6], does not involve a penalty term and simply computes the fluxes by taking the average of the functional limits on each side of the inter-element interfaces Γ_{ij}. Though this option seems attractive, the lack of a penalty term renders the method unstable and may lead to a singular discretization matrix on certain grids. It is therefore clear that the stabilization of the DG methods via the inclusion of a penalty term is crucial. In fact, without it, not only stability is affected, but convergence is degraded or lost [5].

To define the numerical fluxes that will be used in this paper, it is convenient to introduce, for $q \in Q^h$, $u \in U^h$, and $x \in \Gamma_{ij}$, the mean value operators

$$\{u\}(x) = \frac{1}{2}(u_i(x) + u_j(x)),$$
$$\{q\}(x) = \frac{1}{2}(q_i(x) + q_j(x)),$$

and the associated jump operators

$$[u](x) = \frac{1}{2}(u_i(x) - u_j(x))n_{ij},$$
$$[q](x) = \frac{1}{2}(q_i(x) - q_j(x)) \cdot n_{ij}.$$

Here $(q_k, u_k) = (q, u)|_{T_k}$ and n_{ij} is the unit normal on Γ_{ij} pointing from T_i to T_j. We shall employ the numerical fluxes associated with the method of Brezzi et al. [7], which are

$$\bar{u} = \{u^h\}, \quad \bar{q} = \{q^h\} - \eta[u^h]. \tag{5}$$

These numerical fluxes have been analyzed in [8] in the wider context of LDG (Local Discontinuous Galerkin) methods, and gives a stable, convergent method when $\eta = \mathcal{O}(1/h)$. While there are many other numerical fluxes that has been proposed for DG methods, see e.g., [5], we have chosen to use the Brezzi fluxes (5) because they are simple, stable, and consistent, and give the same rate of convergence (at least for elliptic problems with smooth coefficients) as more elaborate DG methods.

The Primal Formulation

The need to construct approximation spaces for both the potential variable and the velocity variable leads to a relatively large number of degrees of freedom per element. However, it is standard procedure in the literature on DG methods to eliminate

the velocity variable from the discretized equations. This elimination leads to the primal formulation:

$$B^h(u^h, v) = \int_\Omega f v \,\mathrm{d}x, \quad \forall v \in U^h, \tag{6}$$

where the primal form $B^h(\cdot,\cdot)$ is defined by

$$\begin{aligned} B^h(u^h, v) := \textstyle\int_\Omega \nabla u^h \cdot a \nabla v \,\mathrm{d}x + \int_{\partial\mathcal{T}} ([\bar{u} - u^h] \cdot \{a\nabla v\} + \{\bar{q}\} \cdot [v]) \,\mathrm{d}s \\ + \textstyle\int_{\partial\mathcal{T}\setminus\partial\Omega} (\{\bar{u} - u^h\}[a\nabla v] + [\bar{q}]\{v\}) \,\mathrm{d}s, \end{aligned} \tag{7}$$

and $\bar{q} = \bar{q}(u^h, q^h)$ is defined with the understanding that q^h satisfies

$$\begin{aligned} -\textstyle\int_\Omega a^{-1} q^h \cdot p \,\mathrm{d}x = \int_\Omega \nabla u^h \cdot p \,\mathrm{d}x + \int_{\partial\mathcal{T}} [\bar{u} - u^h] \cdot \{p\} \,\mathrm{d}s \\ + \textstyle\int_{\partial\mathcal{T}\setminus\partial\Omega} \{\bar{u} - u^h\}[p] \,\mathrm{d}s. \end{aligned} \tag{8}$$

If the unknowns associated with the velocity variable q^h are numbered sequentially, element by element, then the matrix block that stems from the term on the left hand side of (8) becomes block diagonal. This allows us to perform a Schur-elimination of the discretization matrix to give the reduced form corresponding to $B^h(\cdot,\cdot)$ at a low cost. Thus, to compute u^h using the primal formulation, we eliminate first the velocity variable by Schur-elimination. The next step is to solve (6) for u^h. Finally one obtains an explicit expression for the fluxes by back-solving for q^h in (8).

For the numerical fluxes considered in this paper, we have $\bar{u} = \{u^h\}$. Thus, since $\bar{q}$ is conservative, i.e., unit valued on $\partial\mathcal{T}$, the integral over $\partial\mathcal{T}\setminus\partial\Omega$ in $B^h(u^h, v)$ vanishes, and the primal form reduces to

$$B^h(u^h, v) := \int_\Omega \nabla u^h \cdot a \nabla v \,\mathrm{d}x - \int_{\partial\mathcal{T}} ([u^h] \cdot \{a\nabla v\} - \{\bar{q}\} \cdot [v]) \,\mathrm{d}s. \tag{9}$$

Finally, inserting $\bar{q} = \{q^h\} - \eta[u^h]$ into (9) gives

$$B^h(u^h, v) = \int_\Omega \nabla u^h \cdot a \nabla v \,\mathrm{d}x - \int_{\partial\mathcal{T}} [u^h] \cdot \{a\nabla v\} - (\{q^h\} - \eta[u^h]) \cdot [v] \,\mathrm{d}s. \tag{10}$$

A rigorous analysis of the primal form (10) in the case of polynomial elements can be found in [5]. There it was shown that the bilinear form (10) is bounded and stable, provided that the stabilizing coefficient η is chosen sufficiently large. Hence, the same type of constraint applies to η either we formulate the DG method using the mixed formulation (3)–(4) or the primal formulation (6) and (8) using the primal form (10).

2.2 Finite Element Methods vs. Discontinuous Galerkin Methods

The standard conforming FE discretization of (1) approximates the solution in a finite dimensional subspace V^h of $H^1(\Omega)$. Though $H^1(\Omega)$ is not in general embedded in

$C(\bar{\Omega})$, the discrete FE approximation spaces are. This implies in particular that the corresponding FE methods approximates a possible irregular solution with a continuous one. This continuity assumption can be relaxed, as the non-conforming FE methods do, but they still restrain the solution by putting explicit restrictions on the approximation space. This is in a sense the main difference between FE methods and the DG methods which impose continuity implicitly in a weak sense.

In order to clarify the differences, or perhaps rather the similarities, between FE methods and DG methods for equation (1), we first review the concept behind FE methods. In the standard FE formulation of (1) we define a finite dimensional subspace $U^h \subset H^1(\Omega) \cap C(\bar{\Omega})$ and seek $u \in U_D^h(\Omega) = \{u \in U^h : u = 0 \text{ on } \Gamma_{\mathrm{D}}\}$ such that

$$\int_\Omega (\nabla u^h)^T a \nabla v \,\mathrm{d}x = \int_\Omega f v \,\mathrm{d}x \quad \forall v \in U_D^h.$$

Now, since $U^h \subset C(\bar{\Omega})$ we know that u^h is continuous. Hence, it makes sense to let $\bar{u} = u^h$ in (7). We then deduce that the primal form (7) reduces to

$$B^h(u^h, v) = \int_\Omega (\nabla u^h)^T a \nabla v \,\mathrm{d}x + \int_{\partial\mathcal{T}\backslash\Omega} [\bar{q}]\{v\}. \tag{11}$$

Thus, if the numerical flux $\bar{q}$ is conservative, i.e. if $\bar{q}$ is single valued on $\partial\mathcal{T}\backslash\Omega$, then the last term on the right hand side of (11) vanishes. Thus, for any approximation space Q^h, the primal formulation of DG methods with a conservative numerical flux for the velocity variable and an approximation space $U^h \subset C(\bar{\Omega})$ reduces to the standard FE variational formulation.

Similarly, in mixed FE methods one seeks a solution (q^h, u^h) of the elliptic problem (1) in a finite dimensional subspace $Q_N^h \times U_D^h$ of $H(\mathrm{div}, \Omega) \times \mathrm{L}^2(\Omega)$. The subscripts N and D indicate that functions in Q_N^h and U_D^h satisfy the homogeneous Neumann and Dirichlet conditions on Γ_N and Γ_D respectively. The mixed FE solution is defined by the following mixed formulation:

$$\begin{aligned} \int_\Omega a^{-1} q^h \cdot p \,\mathrm{d}x &= \int_\Omega u^h \nabla \cdot p \,\mathrm{d}x, && \forall p \in Q_N^h, \\ \int_\Omega \nabla \cdot q^h v \,\mathrm{d}x &= \int_\Omega f v \,\mathrm{d}x, && \forall v \in U^h, \end{aligned}$$

where n is the outward unit normal on $\partial\Omega$.

For many standard mixed FE methods for equation (1), such as the Raviart–Thomas method [15], the approximation space for the velocity consists of functions that are continuous across the interfaces Γ_{ij} in the direction of the coordinate unit normal n_{ij}. For this type of methods we have $\int_{\Gamma_{ij}} [q] ds = 0$ for all $\Gamma_{ij} \subset \Gamma$ and $q \in Q^h$. Thus, by setting $\bar{q} = q^h$ on Γ and $\bar{q} \cdot n = 0$ on Γ_N we find that the second equation above transforms, upon integration by parts, to equation (4). Moreover, if the numerical flux $\bar{u}$ for the potential is single-valued on Γ, then the first equation in the mixed formulation coincides with equation (3). This shows that also mixed FE methods for equation (1) can be viewed as special DG methods for which the numerical fluxes are determined by continuity conditions imposed on the approximation

spaces. We may therefore view the DG methods as special FE methods that impose weak continuity of the numerical solution without putting explicit constraints on the approximation space.

3 Multiscale Methods for Elliptic Problems

Many areas of science and engineering face the problem of unresolvable scales. For instance, in porous media flows the permeability of the porous medium is rapidly oscillatory and can span across many orders of magnitude across short distances. By elementary considerations it is impossible to do large scale numerical simulations on models that resolve all pertinent scales down to, e.g., the scale of the pores. The standard way of resolving the issue of unresolvable scales is to build coarse scale numerical models in which small scale variations in the coefficients of the governing differential equations are homogenized and upscaled to the size of the grid blocks. Thus, in this approach small scale variations in the coefficients are replaced with some kind of effective properties in regions that correspond to a grid block in the numerical model.

Multiscale methods have a different derivation and interpretation. In these methods one tries to derive coarse scale equations that incorporate the small scale variations in a more consistent manner. Here we present three different types of multiscale methods; the multiscale FE method (MsFEM) developed by Hou and Wu [12], the mixed MsFEM developed by Chen and Hou [9], and a new class of multiscale DG methods (MsDGM). In these multiscale methods one does not alter the differential coefficients, but instead one constructs coarse scale approximation spaces that reflect subgrid structures in a way which is consistent with the local property of the differential operator. They are therefore more amenable to mathematical analysis, and provides a more flexible approach to solving partial differential equations with multiple scales.

One of the motives for using multiscale methods is reduced complexity. Hence, by introducing a rigorous mathematical formalism where one derives a coarse grid model in which subgrid oscillations in the elliptic coefficients are handled in a mathematical consistent manner, one aims toward a reward in terms of computational efficiency. The computational complexity of the methods proposed below scales linearly with the number of cells in the subgrid model. Hence, the complexity is comparable to the (theoretical) complexity of solving the full system of equations at the subgrid level using an efficient multigrid method. Thus, for these methods it appears that we do not gain much. However, for multiscale problems there are additional considerations.

First, in equations of the form (1) that arise from flows in porous media, the elliptic coefficient function $a(x)$ can vary more than 10 orders of magnitude across short distances. With this extreme span of scales it can be very difficult to obtain linear complexity, or even convergence, using multigrid methods, in particular for linear systems that arise from mixed FE methods. In multiscale methods, like the MsFEM, variations in the coefficients that occur on a subgrid scale appear in the

corresponding linear system only as quantities that are integrated over coarse grid blocks. This implies that the impact of the oscillating coefficients on the condition number of the linear system is less severe than for the associated linear system at the subgrid level. In other words, by using a multiscale method we are implicitly doing a preconditioning of the system of subgrid equations. As a consequence, the proposed multiscale methods can be used to obtain quite accurate solutions at the subgrid level for elliptic problems with a range of scales that push the limits, or go beyond the capabilities of multigrid methods.

Another arena where the multiscale methods outlined below can prove useful, also from a computational complexity point of view, is multiphase flow simulation. In a sequential IMPES (IMplicit Pressure Explicit Saturation) formulation of the equations governing incompressible flows in porous media, the pressure equation is basically elliptic, and is non-linearly coupled with a set of (fluid) transport equations. This implies that the pressure equation must be solved repeatedly during a multiphase flow simulation. Fortunately, when simulating fluid flows, for instance flow of oil and water in a heterogeneous oil reservoir, the pressure equation is only weakly coupled to the transport equations. This means that the flow velocity field varies slowly in time away from the propagating saturation front. In such situations the base functions for the proposed multiscale methods need only be generated once, or perhaps a few times during the simulation [1]. In other words, all computations at the subgrid level become part of an initial preprocessing step.

3.1 The Multiscale Finite Element Method

We associate with each element T a set of functions $\mu_T^k \in H^{1/2}(\partial T)$ that play the role of Dirichlet boundary conditions. We then define corresponding multiscale base functions ϕ_T^k by

$$\int_T \nabla \phi_T^k \cdot a \nabla v \, \mathrm{d}x = 0, \quad \forall v \in H_0^1(T), \tag{12}$$

and the associated boundary conditions

$$\begin{aligned} \phi_T^k &= \mu_T^k, && \text{on } \partial \mathrm{T} \backslash \partial \Omega, \\ \phi_T^k &= 0, && \text{on } \Gamma_\mathrm{D} \cap \partial \mathrm{T}, \\ -a \nabla \phi_T^k \cdot n &= 0, && \text{on } \Gamma_\mathrm{N} \cap \partial \mathrm{T}. \end{aligned}$$

To ensure that the base functions are continuous, and hence belong to $H^1(\Omega)$, we require that $\mu_{T_i}^k = \mu_{T_j}^k$ on all non-degenerate interfaces Γ_{ij}. The MsFEM now seeks $u^{\mathrm{ms}} \in U^{\mathrm{ms}} = \mathrm{span}\{\phi^{\mathrm{k}} : \phi^{\mathrm{k}} = \sum_{\mathrm{T}} \phi_{\mathrm{T}}^{\mathrm{k}}\}$ such that

$$\int_\Omega \nabla u^{\mathrm{ms}} \cdot a \nabla v \, \mathrm{d}x = \int_\Omega f v \, \mathrm{d}x \quad \forall v \in U^{\mathrm{ms}}. \tag{13}$$

Since the base functions are determined by the homogeneous equation (12), it is clear that the properties of the approximation space U^{ms}, and hence of the accuracy of the

multiscale solution u^{ms}, is determined by the boundary data μ_T^k for the multiscale base functions ϕ_T^k.

In [12, 13] it was shown using homogenization theory that for elliptic problems in two dimensions with two-scale periodic coefficients, the solution u^{ms} tends to the correct homogenized solution in the limit as the scale of periodicity tends to zero, $\epsilon \to 0$. For a positive scale of periodicity, a relation between ϵ and the discretization scale h was established for linear boundary conditions. Moreover, using multiscale expansion of the base functions they showed that with linear boundary conditions μ_T^k at the interfaces, the resulting solution exhibits a boundary layer near the cell boundaries and satisfies

$$\|u - u^{\mathrm{ms}}\|_{L^2(\Omega)} = \mathcal{O}(h^2 + \epsilon/h).$$

This shows that when ϵ and h are of the same order, a large resonance error is introduced. To reduce the resonance effect, which is caused by improper boundary conditions, Hou and Wu introduced also an oversampling technique motivated by the observation that the boundary layer has a finite thickness of order $O(\epsilon)$. However, for further details about this oversampling technique we refer the reader to the article by Hou and Wu [12].

3.2 The Mixed Multiscale Finite Element Method

For each interface Γ_{ij}, define a Neumann boundary condition $\nu_{ij} \in H^{-1/2}(\Gamma_{ij})$ with $\int_{\Gamma_{ij}} \nu_{ij}\,\mathrm{d}s = 1$. Furthermore, for each interface let the corresponding base function ψ_{ij} for the mixed MsFEM be defined by

$$\begin{aligned} \psi_{ij} &= -a\nabla\phi_{ij}, \quad \text{in } \mathrm{T_i} \cup \mathrm{T_j}, \\ \nabla\cdot\psi_{ij} &= \begin{cases} |T_i|^{-1} & \text{in } \mathrm{T_i}, \\ -|T_j|^{-1} & \text{in } \mathrm{T_j}, \end{cases} \end{aligned} \tag{14}$$

and the following boundary conditions:

$$\begin{aligned} \psi_{ij}\cdot n_{ij} &= \nu_{ij}, && \text{on } \Gamma_{\mathrm{ij}}, \\ \phi_{ij} &= 0, && \text{on } \partial(\mathrm{T_i} \cup \mathrm{T_j}) \cap \Gamma_{\mathrm{D}}, \\ \psi_{ij}\cdot n &= 0, && \text{on } \partial(\mathrm{T_i} \cup \mathrm{T_j}) \backslash (\Gamma_{\mathrm{ij}} \cup \Gamma_{\mathrm{D}}). \end{aligned}$$

Here n_{ij} is the coordinate unit normal to Γ_{ij} pointing from T_i to T_j and n is the outward unit normal on $\partial(T_i \cup \Gamma_{ij} \cup T_j)$. We now define $Q^{\mathrm{ms}} = \mathrm{span}\{\psi_{\mathrm{ij}} : \Gamma_{\mathrm{ij}} \subset \Gamma\}$ and seek $(q^{\mathrm{ms}}, u) \in Q^{\mathrm{ms}} \times \mathcal{P}_0(\mathcal{T})$ which solves

$$\begin{aligned} \int_\Omega a^{-1} q^{\mathrm{ms}} \cdot p\,\mathrm{d}x &= \int_\Omega u\,\nabla\cdot p\,\mathrm{d}x, && \forall p \in Q^{\mathrm{ms}}, \\ \int_\Omega v \nabla\cdot q^{\mathrm{ms}}\,\mathrm{d}x &= \int_\Omega f v\,\mathrm{d}x, && \forall v \in \mathcal{P}_0(\mathcal{T}). \end{aligned}$$

Again we see that the method is determined by the local boundary conditions for the base functions.

It is also possible to choose the right hand side of the equations (14) differently, and in some cases it would be natural not to do so. For instance, in reservoir simulation the right hand side of equation (1) represent wells and wells give rise to source terms that are nearly singular. For simulation purposes it is important that the velocity field is mass conservative. To this end, the right hand side of equation (14) in the well blocks must be replaced with a scaled source term at the well location, see [1] for further details.

A rigorous convergence analysis for the mixed MsFEM has been carried out in [9] for the case of two-scale periodic coefficients using results from homogenization theory. There it was shown that

$$\|q - q^{\mathrm{ms}}\|_{H(\mathrm{div},\Omega)} + \|u - u^{\mathrm{ms}}\|_{L^2(\Omega)} = \mathcal{O}\left(h + \sqrt{\epsilon/h}\right).$$

Hence, again we see that a large resonance error is introduced when $\epsilon/h = \mathcal{O}(1)$. As for the MsFEM method, the possibility of using oversampling as a remedy for resonance errors was explored, and it was shown that oversampling can indeed be used to reduce resonance errors caused by improper boundary conditions. The need for oversampling strategies to reduce resonance errors is, however, a drawback with the MsFEMs since oversampling leads to additional computational complexity.

3.3 A Multiscale Discontinuous Galerkin Method

We now exploit the relationship between DG methods and FE methods that was established in Sect. 2.2. To derive the MsDGM proposed below, we "merge" first the approximation spaces constructed in the original and mixed MsFEMs to create a pair of approximation spaces for the MsDGM. Thus, select suitable boundary conditions $\mu_T^k \in H^{1/2}(\partial T)$ and $\nu_{ij} \in H^{-1/2}(\Gamma_{ij})$ and define base functions ϕ_T^k and ψ_{ij} by (12) and (14) respectively. The approximation spaces for the MsDGM are then defined by

$$U^{\mathrm{ms}} = \mathrm{span}\{\phi^{\mathrm{k}} : \phi^{\mathrm{k}} = \sum_{\mathrm{T}} \phi_{\mathrm{T}}^{\mathrm{k}}\} \quad \text{and} \quad \mathrm{Q}^{\mathrm{ms}} = \mathrm{span}\{\psi_{\mathrm{ij}} : \Gamma_{\mathrm{ij}} \subset \Gamma\}.$$

Thus, the corresponding DG method, henceforth called the MsDGM, reads:

Find $(q^{\mathrm{ms}}, u^{\mathrm{ms}}) \in Q^{\mathrm{ms}} \times U^{\mathrm{ms}}$ so that for each $T \in \mathcal{T}$ we have

$$\int_T a^{-1} q^{\mathrm{ms}} \cdot p \,\mathrm{d}x = \int_T u^{\mathrm{ms}} \nabla \cdot p \,\mathrm{d}x - \int_{\partial T} \bar{u} p \cdot n_T \,\mathrm{d}s, \qquad \forall p \in Q^{\mathrm{ms}}, \tag{15}$$

$$\int_T q^{\mathrm{ms}} \cdot \nabla v \,\mathrm{d}x = -\int_T f v \,\mathrm{d}x + \int_{\partial T} v \bar{q} \cdot n_T \,\mathrm{d}s, \qquad \forall v \in U^{\mathrm{ms}}. \tag{16}$$

In addition to the selection of boundary conditions for the base functions, this method is determined by the choice of numerical fluxes. As indicated in Sect. 2.1 we limit our study to the numerical fluxes (5) of Brezzi et al.

We observe that MsDGMs have much in common with the mortar FE methods. Indeed, here as in the mortar methods, we construct the base functions locally in a

manner which corresponds to the underlying partial differential equation, and glue the pieces together using a weak formulation at the interfaces. The new element here is that we derive the above formulation directly from the original and mixed MsFEMs.

Apart for imposing inter-element continuity weakly, the MsDGMs differ from the MsFEMs by using multiscale approximation spaces for both the velocity variable and the potential variable. Another motive for introducing a new multiscale method for elliptic problems is that the accuracy of MsFEMs solutions can be sensitive to the boundary conditions for the base functions. Indeed, previous numerical experience [1, 2] shows that the MsFEMs with simple boundary conditions may produce solutions with poor accuracy when strong heterogeneous features penetrate the inter-element interfaces. Thus, by introducing a MsDGM we aim toward a class of multiscale methods that are less sensitive to resonance errors caused by improper boundary conditions for the multiscale basis functions.

3.4 On the Selection of Boundary Conditions for the MsFEM

Consider the following homogeneous boundary value problem,

$$\begin{aligned} (a(x)u_x)_x &= f, && \text{in } \Omega = (0,1), \\ u &= 0, && \text{on } \partial\Omega = \{0,1\}. \end{aligned} \tag{17}$$

and let $\mathbf{x} = \{x_i : 0 = x_0 < x_1 < \ldots < x_N = 1\}$ be a corresponding set of finite element nodal points. Now let $V = H_0^1(\Omega\backslash\mathbf{x})$ and define

$$U = \{u \in H_0^1(\Omega) : (a(x)u_x)_x = 0 \text{ weakly on } \Omega\backslash\mathbf{x},\ u = 0 \text{ on } \partial\Omega\}.$$

Then it is easy to see that $H_0^1(\Omega) = U + V$ and that U and V are orthogonal with respect to the energy norm, i.e.,

$$a(u,v) := \int_\Omega a(x)u_x v_x \,\mathrm{d}x = 0 \quad \forall u \in U, \forall v \in V.$$

Thus, since U^{ms} coincides with U, it follows from the projection property of the FE method that $u^{\mathrm{ms}} = u_I$ where u_I is the interpolant of the exact solution u on $\mathbf{x}$ in $U^{\mathrm{ms}} = U$. This property is due to the fact that there is no resonance error caused by improper boundary conditions and implies that the conforming MsFEM induces an ideal domain decomposition preconditioner for elliptic problems in one spatial dimension.

In higher dimensions the choice of boundary conditions is no longer insignificant. In fact, the MsFEM may be viewed as an extension operator acting on Γ. Hence, the restriction of the solution u^{ms} to Γ must lie in the space spanned by the boundary conditions for the base functions. To clarify the relation between the approximation properties for the MsFEM and the selection of boundary conditions, we consider the following homogeneous boundary value problem: Find $u \in H_0^1(\Omega)$ such that

$$a(u,v) := \int_\Omega \nabla u \cdot a(x)\nabla v \,\mathrm{d}x = \int_\Omega f v \,\mathrm{d}x, \quad \forall v \in H_0^1(\Omega).$$

Now, let $M = H_0^1(\Omega)|_\Gamma$ and define the following extension operator

$$H : M \to H_0^1(\Omega), \quad a(H\mu, v) = 0, \quad \forall v \in H_0^1(\Omega \backslash \Gamma). \tag{18}$$

This extension operator induces a norm on M defined by $\|\mu\|_M^2 = a(H\mu, H\mu)$. Clearly, by definition we find that U^{ms} is a subspace of $W = H(M)$, the space of generalized harmonic functions. In fact, if $M^{\mathrm{ms}} = \mathrm{span}\{\mu_{\mathrm{T}}^{\mathrm{k}}\}$, then $M^{\mathrm{ms}} \subset M$ and $U^{\mathrm{ms}} = H(M^{\mathrm{ms}})$. Thus, since u^{ms} in (13) is the orthogonal projection of the exact solution u onto U^{ms} with respect to $a(\cdot,\cdot)^{1/2}$, it follows that $\mu^{\mathrm{ms}} = u^{\mathrm{ms}}|_\Gamma$ is the orthogonal projection of $\mu = u|_\Gamma$ onto M^{ms} with respect to $\|\cdot\|_M$. This shows that the MsFEM also defines an orthogonal projection onto the space of interface variables with respect to the relevant norm $\|\cdot\|_M$, and hence induces an optimal coarse solver for non overlapping domain decomposition methods. The properties of the MsFEM as a coarse solver in domain decomposition methods has been further analyzed in [2, 3].

4 Numerical Results

Let $\Omega = (0,1) \times (0,1)$ be the computational domain. A uniform finite element mesh $\mathcal{T}$ is constructed by dividing Ω into $N \times N$ squares. The multiscale methods further subdivide each element into $M \times M$ square elements. A reference solution is computed on the full resolved $NM \times NM$ mesh. The global boundary conditions are specified by setting $\Gamma_D = \partial\Omega$ and $\Gamma_N = \emptyset$.

We will test six methods, three monoscale numerical methods and three multiscale methods. The first monoscale method is the FE method (FEM) on quadrilateral grids with bilinear basis functions. The second method is the Raviart–Thomas mixed FEM [15] (MFEM) of lowest order on regular quadrilateral grids. This method uses piecewise constant basis functions for the potential and piecewise linear basis functions for the velocity. The last monoscale method is the DG method (DGM) which uses bilinear basis functions for potential and linear basis functions for the velocity. These monoscale methods will be compared with their multiscale variants defined in Sect. 3, i.e., with the MsFEM, the mixed MsFEM (MsMFEM), and the MsDGM. For these multiscale methods we use the FEM with bilinear basis functions to compute the base functions that span the approximation space U^{ms} for the potential variable u and the Raviart–Thomas mixed FEM to compute the basis functions that span the approximation space Q^{ms} for the velocity variable q. Finally, the reference solution is computed using the Raviart–Thomas mixed FEM. We assess the accuracy of the tested methods with the weighted error measures

$$E(u_h) = \frac{\|u_h - u_r\|_2}{\|u_r\|_2}, \qquad E(q_h) = \frac{1}{2}\left(\frac{\|q_h^x - q_r^x\|_2}{\|q_r^x\|_2} + \frac{\|q_h^y - q_r^y\|_2}{\|q_r^y\|_2}\right).$$

Here $\|\cdot\|_2$ is the $L^2(\Omega)$-norm, the subscript h denotes computed solutions, the subscript r refers to the reference solution and the superscripts x and y signifies velocity components. When comparing velocity fields we do not include the FEMs since these methods are not conservative.

4.1 Subscale Oscillations

We apply the methods to equations (1) with

$$a(x,y) = \frac{2 + P\sin(2\pi x/\epsilon)}{2 + P\sin(2\pi y/\epsilon)} + \frac{2 + P\sin(2\pi y/\epsilon)}{2 + P\cos(2\pi x/\epsilon)},$$
$$f(x,y) = 2\pi^2 \cos(\pi x)\cos(\pi y).$$

This type of coefficients $a(x,y)$ give rise to spurious oscillations in the velocity field, and the source term $f(x,y)$ exerts a low frequent force. We shall fix $P = 1.8$, $NM = 512$ and $\epsilon = 1/64$ for our numerical test cases. We thus get significant subgrid variation for $N < 64$ while the resonance is greatest at $N = 64$. When $N > 64$ the characteristic scale of variation is resolved by the coarse mesh and the use of multiscale methods are no longer necessary.

Table 1. Potential errors for oscillatory coefficients. For the DGM and the MsDGM, the numbers presented correspond to the choice of η that gave the smallest error

N	M	FEM	MFEM	DGM	MsFEM	MsMFEM	MsDGM
8	64	0.9355	1.150	0.6905	0.1161	0.3243	0.08239
16	32	1.043	1.100	0.5674	0.03845	0.1733	0.03776
32	16	1.072	1.086	0.4998	0.02862	0.1127	0.06817
64	8	0.7119	0.712	0.7117	0.04422	0.1508	0.1269

Table 2. Relative velocity errors for oscillatory coefficients. For the DG methods the numbers presented correspond to the choice of η that gave the smallest error

N	M	MFEM	DGM	MsMFEM	MsDGM
8	64	0.5533	0.6183	0.2985	0.4291
16	32	0.5189	0.5388	0.2333	0.2842
32	16	0.5093	0.5144	0.2377	0.2579
64	8	0.5058	0.5079	0.2866	0.3177

Table 1 shows errors $E(u^h)$ in the potential for all the methods. We see that none of the monoscale methods perform particularly well, as they cannot pick up subgrid variations in the coefficients, but the DGM is somewhat more accurate than the other methods. The multiscale methods, on the other hand, generate quite accurate potential fields. The MsFEM is most accurate here, but MsDGM is nearly as accurate, and for very coarse meshes it is the most accurate method. The least accurate multiscale method is the MsMFEM. This is probably due to the fact that piecewise constant functions are used to approximate the potential. The results shown in Table 2 demonstrate that the monoscale methods tend to give more accurate velocity

fields than potential fields, but we still see that the multiscale methods give much higher accuracy. We observe also that for this test case the MsMFEM gives more accurate velocity fields than the MsDGM.

The accuracy of the DG methods depend on the parameter η in (5). The results in Table 1 and Table 2 correspond to the value of $\eta = \eta^*$ that produced the best solutions. Since we do not know a priori what η^* is, it is natural to ask how the error behaves as a function of η, and, in particular, how sensitive the DG methods are to the penalty parameter η. We have therefore plotted $E(u_h)$ and $E(q_h)$ for both the DG method and the MsDGM in Figs. 1 and 2 as functions of η. We see that the DG method only converges for a succinct choice of η, except for $N = 64$. In contrast, the MsDGM converges with good accuracy for sufficiently large η. These plots thus demonstrate that; (1): for elliptic problems with oscillating coefficients the MsDGM is less sensitive to η than the monoscale DG methods, and (2): the convergence behavior for the MsDGM seem to be in accordance with the convergence theory for DG methods for elliptic problems with smooth coefficients.

4.2 Random Coefficients

In the second experiment the elliptic coefficient function $a(x, y)$ take random values in the interval $(0, 1)$. Thus, for each grid cell in the fine mesh the value of a is selected at random from this interval. We now only consider the multiscale methods, and compare the MsDGM with the MsFEM and the MsMFEM. The corresponding errors are shown in Table 3. We observe that for this test case the MsDGM generates the by far most accurate potential field, in fact, by almost an order of magnitude. The MsMFEM still produces the most accurate velocity field, but the MsDGM produces a velocity field with comparable accuracy. These results are representative for the results we obtained for a variety of different random coefficient functions. Again the parameter η for the MsDGM numerical flux function $\bar{q}$ was attempted optimized in order to give best results.

Table 3. Potential errors $E(u_h)$ (left) and Velocity errors $E(q_h)$ (right) for an elliptic problem with random coefficients

N	M	MsFEM	MsMFEM	MsDGM	MsMFEM	MsDGM
8	64	0.4458	0.3290	0.1394	0.3375	0.4849
16	32	0.3827	0.1839	0.07163	0.2851	0.3716
32	16	0.3589	0.1510	0.03766	0.2941	0.3472
64	8	0.3335	0.2074	0.02539	0.3346	0.3624

The results in Table 3 indicate that the MsDGM may be more robust than the MsFEM. Unfortunately, for this case the MsDGM was more sensitive to η than what we observed in Sect. 4.1, and choosing η too large can deteriorate the convergence, see Fig. 3. However, the optimal η for potential ($\sim 13,\ \sim 34,\ \sim 83$ and ~ 188 for

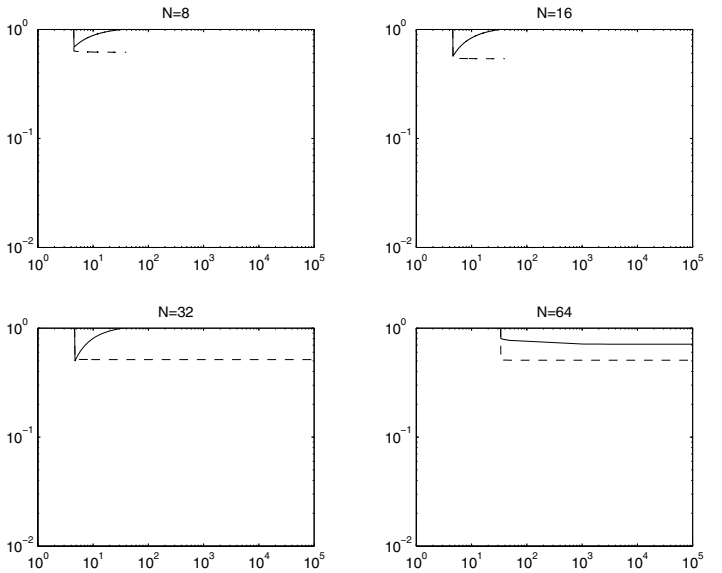

Fig. 1. Errors induced by the DG method as functions of η. The solid line is the potential error, and the dashed line is the velocity error

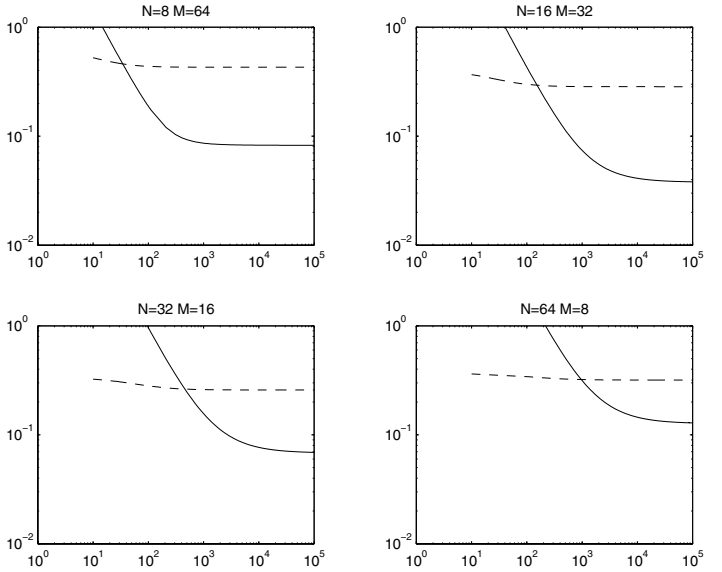

Fig. 2. Errors induced by the MsDGM as functions of η. The solid line is the potential error, and the dashed line is the velocity error. Note that the error decreases monotonically as η increases, and that the method converges for $\eta > \mathcal{O}(1/h)$

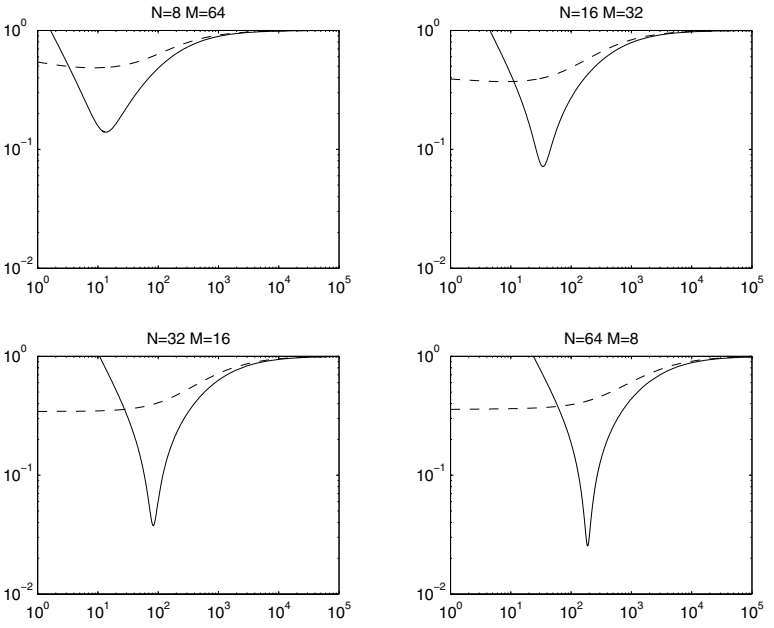

Fig. 3. Logarithmic plot of errors for the MsDGM for random coefficients. The plots should be compared with the results depicted in Fig. 2

$h = 8,\ 16,\ 32$ and 64 respectively) still scales like $\mathcal{O}(1/h)$. This suggest that good accuracy should be obtained by choosing $\eta \sim \alpha/h$ for some fixed $\alpha \sim \mathcal{O}(1)$.

5 Concluding Remarks

In this paper, we have used approximation spaces for two different multiscale finite element methods in order to develop a multiscale discontinuous Galerkin method for elliptic problems with multiple scale coefficients. Unlike the multiscale finite element methods, the multiscale discontinuous Galerkin method introduced in this paper provides detailed solutions for both velocity and potential that reflect fine scale structures in the elliptic coefficients. This makes the multiscale discontinuous Galerkin method an attractive tool for solving, for instance, pressure equations that arise from compressible flows in heterogeneous porous media. Indeed, in compressible flow simulations it is not sufficient to resolve the velocity field well, an accurate pressure field is also needed.

Numerical comparisons with both monoscale- and multiscale methods have been given. The results show that monoscale numerical methods are inadequate when it comes to solving elliptic problems with multiple scale solutions. We have further demonstrated that the multiscale discontinuous Galerkin method produce solutions

with comparable or higher accuracy than solutions produced by corresponding multiscale finite element methods. To summarize the results for the multiscale methods, we plot errors for all the multiscale methods in Fig. 4. This figure shows that the velocity solutions obtained with the multiscale discontinuous Galerkin method have comparable accuracy with the velocity solutions obtained with the corresponding mixed multiscale finite element method. The potential solutions produced by the multiscale discontinuous Galerkin method, on the other hand, are equally or more accurate than the potential solutions obtained with both of the multiscale finite element methods.

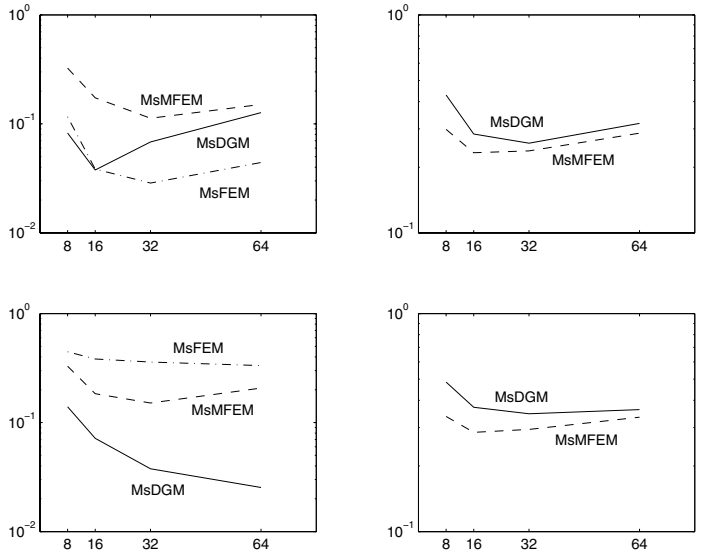

Fig. 4. Plot of the errors as functions of grid size for oscillatory (top) and random coefficients (bottom) respectively. The left figures show potential errors, and the right figures show the velocity errors. The MsDGM is the solid line, the MsMFEM is the dashed line, and the MsFEM is the dashed and dotted line

In the present paper we have not provided any convergence theory, but it is likely that convergence results can be obtained using results from homogenization theory in conjunction with the convergence theory for discontinuous Galerkin methods for elliptic problems with smooth coefficients. However, since the discontinuous Galerkin methods appear to give comparable accuracy to the multiscale mixed finite element methods for which error estimates based on the homogenization theory have been established, one can expect the discontinuous Galerkin methods to enjoy similar error estimates. We have also shown that the multiscale discontinuous Galerkin method appears to converge for values of the penalty parameter η in the numerical flux function that is in accordance with the convergence theory for Galerkin methods for elliptic

problems with smooth coefficients. A rigorous convergence analysis of the multiscale discontinuous Galerkin methods is a topic for further research.

Acknowledgments

We would like to thank Kenneth H. Karlsen and Ivar Aavatsmark for useful comments. The second author would also like to thank the Research Council of Norway for financial support.

References

1. J. Aarnes, On the use of a mixed multiscale finite element method for greater flexibility and increased speed or improved accuracy in reservoir simulation, Multiscale Model. Simul., **2**, 421–439, (2004).
2. J. Aarnes, Efficient domain decomposition methods for elliptic problems in heterogeneous porous media, to appear in Comput. Vis. Science.
3. J. Aarnes, T. Y. Hou, Multiscale domain decomposition methods for elliptic problems with high aspect ratios, Acta Math. Appl. Sinica, **18**, 63–76, (2002).
4. D. N. Arnold, An Interior Penalty Finite Element Method with Discontinuous Elements, SIAM J. Numer. Anal., **19**, 742–760, (1982).
5. D. N. Arnold, F. Brezzi, B. Cockburn, L. D. Marini, Unified Analysis of Discontinuous Galerkin Methods, SIAM J. Numer. Anal., **39**, 1749–1779 (2002).
6. F. Bassi, S. Rebay, A High-Order Accurate Discontinuous Finite Element Method for the Numerical Solution of the Compressible Navier Stokes Equations, J. Comput. Phys., **131**, 267–279, (1997).
7. F. Brezzi, G. Manzini, D. Marini, P. Pietra, A. Russo, Discontinuous Finite Elements for Diffusion Problems, in Atti Convegno in onore di F. Brioschi (Milan 1997), Instituto Lombardo, Accademia di Scienze e Lettere, Milan, Italy, 197–217, (1999).
8. P. Castillo, B. Cockburn, I. Perugia, D. Schötzau, An a priori error analysis of the Local Discontinuous Galerkin Method for Elliptic Problems, SIAM J. Numer. Anal., **38**, 1676–1706, (2000).
9. Z. Chen and T. Y. Hou, A mixed multiscale finite element method for elliptic problems with oscillating coefficients, Math. Comp., **72**, 541–576, (2003).
10. B. Cockburn, G. Karniadakis, C.-W. Shu (eds). Discontinuous Galerkin Methods. Theory, Computation and Applications, Lect. Notes Comput. Sci. Eng., **11**, Springer-Verlag, Heidelberg, (2000).
11. D. Douglas, Jr, T. Dupont, Interior Penalty Procedures for Elliptic and Parabolic Galerkin Methods, Lect. Notes Phys., **58**, Springer-Verlag, Berlin, (1976).
12. T. Y. Hou, X.-H. Wu, A Multiscale Finite Element Method for Elliptic Problems in Composite Materials and Porous Media, J. Comput. Phys., **134**, 169–189, (1997).
13. T. Y. Hou, X.-H. Wu, Z. Cai, Convergence of a Multiscale Finite Element Method for Elliptic Problems with Rapidly Oscillating Coefficients, Math. Comp, **68**, 913-943, (1999).
14. J.-L. Lions, Problèmes aux limites non homogènes à donées irrégulières: Une méthod d'approximation, Num. Anal. Part. Diff. Eqn. (C.I.M.E. 2 Ciclo, Ispra, 1967), Edizioni Cremonese, Rome, 283–292, (1968).
15. P. A. Raviart and J. M. Thomas, A mixed finite element method for second order elliptic equations, Mathematical Aspects of Finite Element Methods (I. Galligani and E. Magenes, eds.), Springer–Verlag, Berlin – Heidelberg – New York, 292–315, (1977).

16. M. F. Wheeler, An Elliptic Collocation-Finite Element Method with Interior Penalties, SIAM J. Numer. Anal., **15**, 152–161, (1978).